Supporting Information

Redox-Switchable Copper(I) Metallogel: A Metal-Organic Material for Selective and Naked-Eye Sensing of Picric Acid

Sougata Sarkar[†], Soumen Dutta[†], Susmita Chakrabarti[‡], Partha Bairi[§] and Tarasankar Pal*[,†]

[†]*Department of Chemistry, Indian Institute of Technology, Kharagpur-721302, India*

[‡]*Department of Chemistry, Jadavpur University, Kolkata-700032, India*

[§]*Department of Chemistry, Indian Association for the Cultivation of Science, Kolkata-700032, India*

E-mail: tpal@chem.iitkgp.ernet.in

Experimental Section

Materials: All reagents were of analytical grade and used without further purification.

Preparation of the gel:

In preparation of the metal-organic hybrid gel, 1 mL aqueous solution of thiourea (3 mg; 0.04 mmol) was placed in a glass vial. To this solution 1 mL aqueous solution of copper(II) chloride was added in varying concentrations from 1.0 to 0.1 molar equivalents with respect to the thiourea concentration. This immediately results in a yellowish-green color solution. After a little shaking to make the solution homogenize, samples were left to stand undisturbed for 1-2 hr. Finally a white color gel was resulted of which the gelation state was avowed by the retardation of flow of the materials upon "inversion of the glass vial". The typical gelation was found to depend on the concentration (equivalent) of $CuCl_2$ added.

Redox-switchability Study:

The redox-switchability study was performed with freshly prepared gel. 0.1 M aqueous solution of the oxidizing agents ($FeCl_3$ or $K_2Cr_2O_7$) and reducing agent (Ascorbic acid) were used in the study.

Sensing of Picric acid:

For this we have introduced nineteen different electron deficient organic compounds (nitro and others) individually. The freshly prepared gel material was incubated with an ethanolic solution

of the selected species (concentration = 0.01 M). Distinguished colour change was only noticed for picric acid. Then again the gel material prepared in ten different glass vial was individually incubated with ten different concentrations of picric acid (50mM to 50μM) solution to study the concentration effect of picric acid on the gel matrix.

Analytical Methods:

Field Emission Scanning Electron Microscopy (FESEM): The morphology of the samples were analyzed by field emission scanning electron microscopy (FESEM) using (Supra 40, Carl Zeiss Pvt. Ltd.) microscope at an accelerating voltage 20 kV. Compositional analysis of the sample was done by an energy dispersive X-ray micro-analyzer (OXFORD ISI 300 EDAX) attached to the scanning electron microscope.

Transmission Electron Microscopy (TEM): TEM analyses of the samples were carried out on a Hitachi H-9000 NAR transmission electron microscope, operating at 80 kV. Samples were prepared by sonicating the gel materials in water and then placing a drop of solution on a carbon coated copper grid followed by solvent evaporation in vacuum.

Polarized Optical Microscope (POM): The micrographs of the samples were obtained from a LEICA DMLM (Germany) optical microscope by transmitted light under crossed Nicol and fitted with JVC-KY-F550E imaging system. A drop of the gel sample from the 'Set I' sample-vial was placed on a glass slide and placed under the microscope.

Fourier Transform Infrared Spectroscopy (FTIR): FTIR spectra of different samples (xerogels and thiourea only) were collected in KBr pellet in reflectance mode with Nexus 870 Thermo-Nicolet instrument coupled with a Thermo-Nicolet Continuum FTIR Microscope.

X-ray diffraction (XRD): XRD patterns of the xerogels ($CuCl_2$: Set I and Set VI; $CuBr_2$: Set I) were recorded in a Philips PW-1710 X-ray diffractrometer (40 kV, 30 mA) using Cu $K\alpha$ radiation (λ=1.5418 Å) in the 2θ range of 1°-70° at a scanning rate of 0.5° min^{-1}.

UV-Visible Spectroscopy: Absorption spectrum was recorded in a Spectrascan UV 2600 spectrophotometer (Chemito, India). The Reflectance spectra were measured using DRS (Diffuse Reflectance Spectra) mode with a Cary model 5000 UV-vis-NIR spectrophotometer.

Fluorescence Spectroscopy: Fluorescence spectrum was recorded in Hitachi (model F-7000) spectrofluorometer.

Raman Spectroscopy: Raman spectrum was obtained with a Renishaw Raman microscope, equipped with the laser source (633 nm) and a Peltier cooled (-70°C) charge coupled device (CCD) camera. A Leica DMLM microscope was attached and was fitted with three objectives (5X, 20X, 50X). For our experiments, the 20X objective was used. Data acquisition time was 30 s. The slit provided a spectral resolution of 1 cm^{-1}.

Rheology: The rheological properties of the gels were achieved with an advanced rheometer (AR 2000, TA Instruments, USA) using cone plate geometry on a peltier plate. The diameter of the plate was 40 mm and angle was 4º with a plate gap of 121μm. The gel samples were placed on the plate and stress sweep experiment at a constant frequency at 25 °C and frequency sweep measurements at a constant stress in the linear viscoelastic range were carried out to get the storage or elastic modulus (G′) and loss or viscous modulus (G″) values of the gel materials.

Table S1. DFT optimized energy of HOMO and LUMO of electron deficient receptors

Entry	Receptors	Energy of HOMO (hartree)	Energy of LUMO (hartree)
1	Benzoic acid	-0.2646	-0.05712
2	Salicylic acid	-0.23596	-0.06218
3	2-nitropropane	-0.29369	-0.08727
4	Nitromethane	-0.30107	-0.09505
5	Phthalic acid	-0.26684	-0.10028
6	4-nitrophenol	-0.26225	-0.10148
7	4-nitrotoluene	-0.27597	-0.10225
8	2-nitrotoluene	-0.27263	-0.10262
9	4-nitrophenyl acetic acid	-0.28258	-0.10586
10	Nitrobenzene	-0.28471	-0.10675
11	3-nitrobenzoic acid	-0.2972	-0.11575
12	4-nitrobenzoic acid	-0.29672	-0.12468
13	2,4-dinitrotoluene	-0.30673	-0.12746
14	3,5-dinitrosalicylic acid	-0.29682	-0.12882
15	4-nitrobenzaldehyde	-0.28307	-0.13025
16	1,3-dinitrobenzene	-0.3165	-0.13367
17	3-nitrophthalic acid	-0.28581	-0.13749
18	2,4-dinitrophenol	-0.29162	-0.14375
19	Picric acid	-0.2889	-0.14691

Surfaces

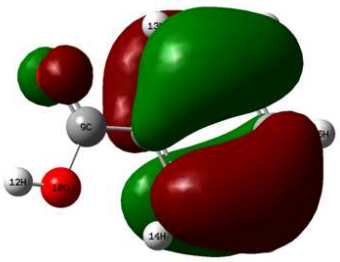

Benzoic Acid

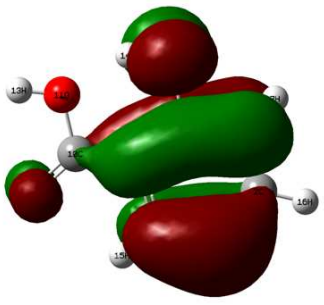

Salicylic Acid

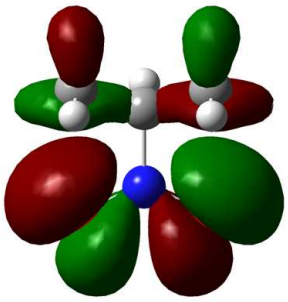

2-nitropropane

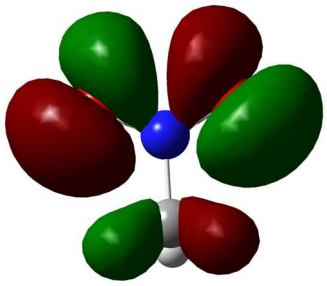

Nitromethane

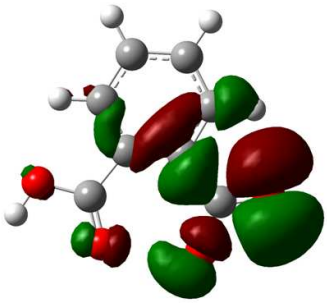

Phthalic acid

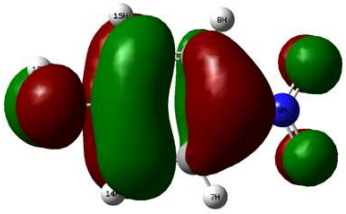

4-nitrophenol

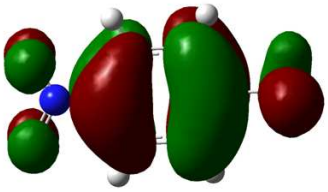

4-nitrotoluene

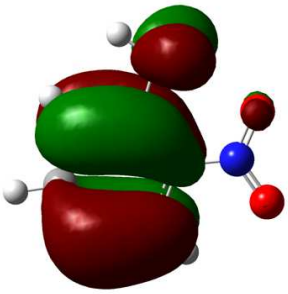

2-nitrotoluene

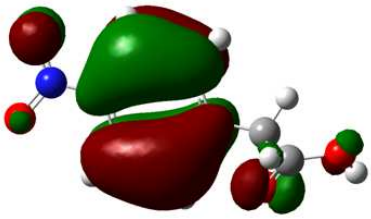

4-nitrophenyl acetic acid

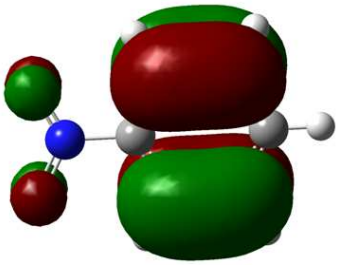

Nitrobenzene

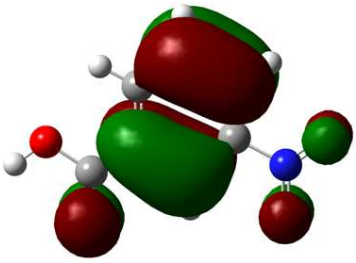

3-Nitrobenzoic acid

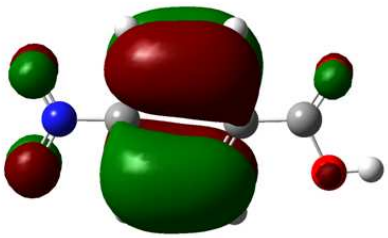

4-Nitrobenzoic acid

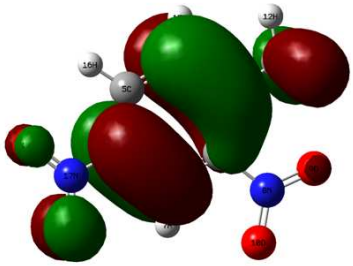

2,4-dinitrotoluene

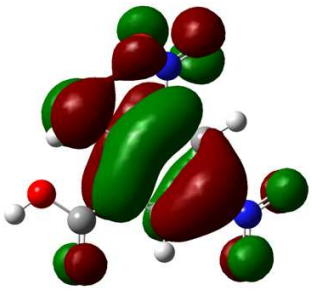

3,5-dinitrosalicylic acid

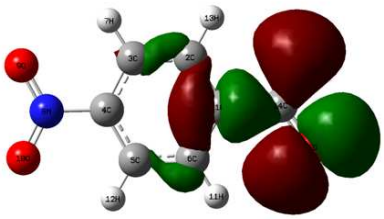

4-Nitrobenzaldehyde

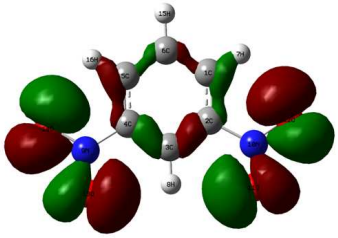

1,3-dinitrobenzene

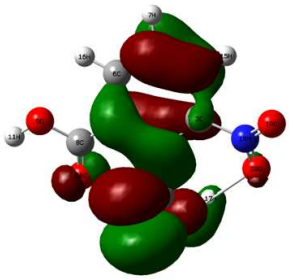

3-nitrophthalic acid

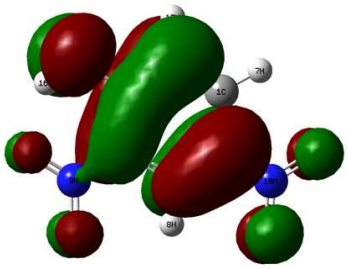

2,4-dinitrophenol

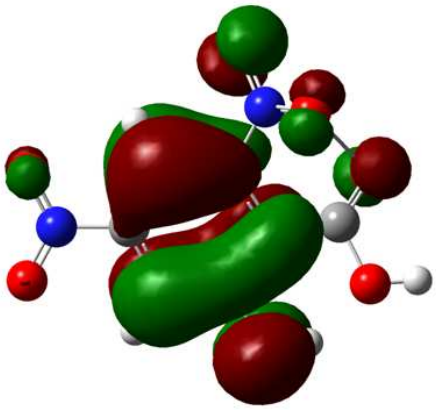

Picric acid

Reference

Frisch, M. J.; Trucks, G. W.; Schlegel, H. B.; Scuseria, G. E.; Robb, M. A.; Cheeseman, J. R.; Scalmani, G.; Barone, V.; Mennucci, B.; Petersson, G. A.; Nakatsuji, H.; Caricato, M.; Li, X.; Hratchian, H. P.; Izmaylov, A. F.; Bloino, J.; Zheng, G.; Sonnenberg, J. L.; Hada, M.; Ehara, M.; Toyota, K.; Fukuda, R.; Hasegawa, J.; Ishida, M.; Nakajima, T.; Honda, Y.; Kitao, O.; Nakai, H.; Vreven, T.; Montgomery, J. A., Jr.; Peralta, J. E.; Ogliaro, F.; Bearpark, M.; Heyd, J. J.; Brothers, E.; Kudin, K. N.; Staroverov, V. N.; Kobayashi, R.; Normand, J.; Raghavachari, K.; Rendell, A.; Burant, J. C.; Iyengar, S. S.; Tomasi, J.; Cossi, M.; Rega, N.; Millam, J. M.; Klene, M.; Knox, J. E.; Cross, J. B.; Bakken, V.; Adamo, C.; Jaramillo, J.; Gomperts, R.; Stratmann, R. E.; Yazyev, O.; Austin, A. J.; Cammi, R.; Pomelli, C.; Ochterski, J. W.; Martin, R. L.; Morokuma, K.; Zakrzewski, V. G.; Voth, G. A.; Salvador, P.; Dannenberg, J. J.; Dapprich, S.; Daniels, A. D.; Farkas, O.; Foresman, J. B.; Ortiz, J. V.; Cioslowski, J.; Fox, D. J. *Gaussian 09*, revision A.02; Gaussian, Inc.: Wallingford, CT, 2009.

Results and discussion

FTIR and Raman analyses

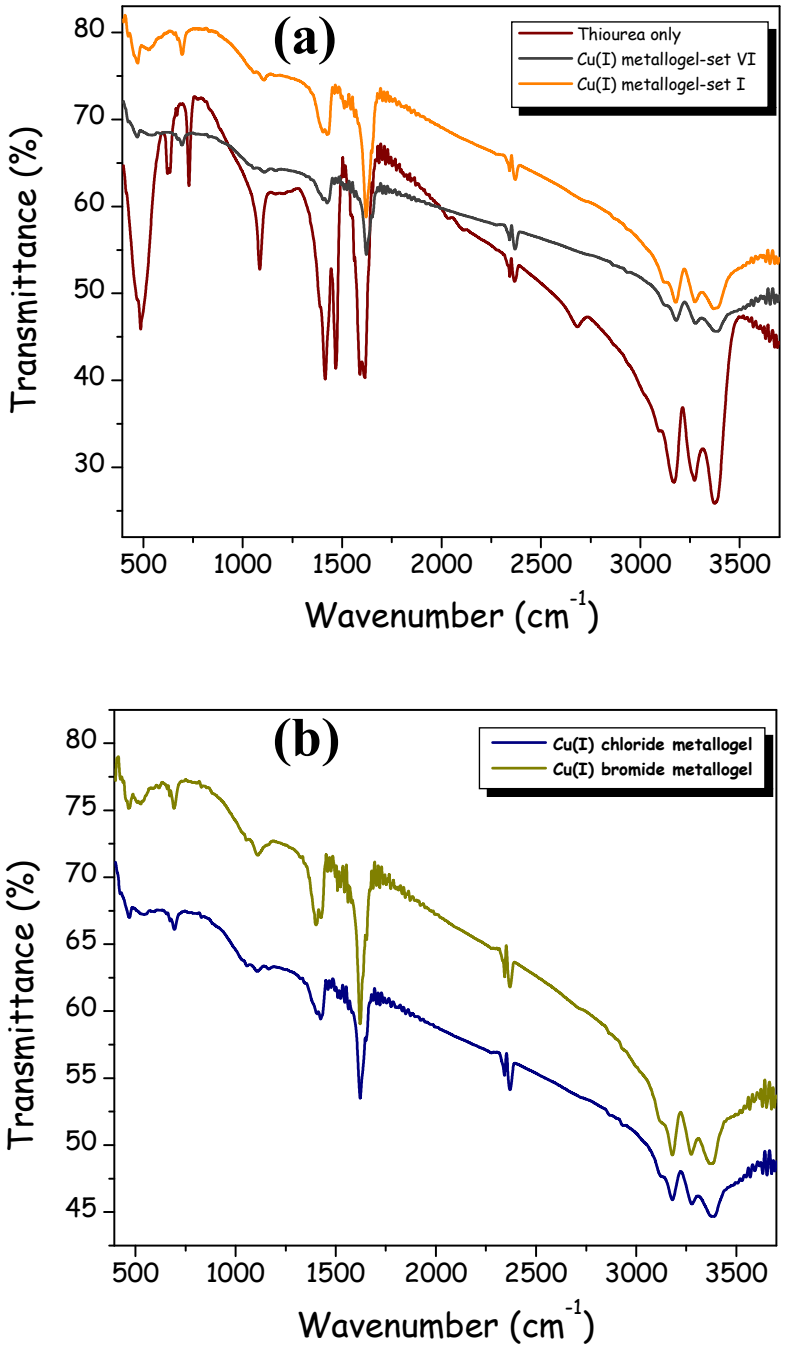

Figure S1. FTIR spectra of (a) thiourea and Cu(I) chloride metallogels of two different compositions and (b) Cu(I) chloride and bromide metallogels.

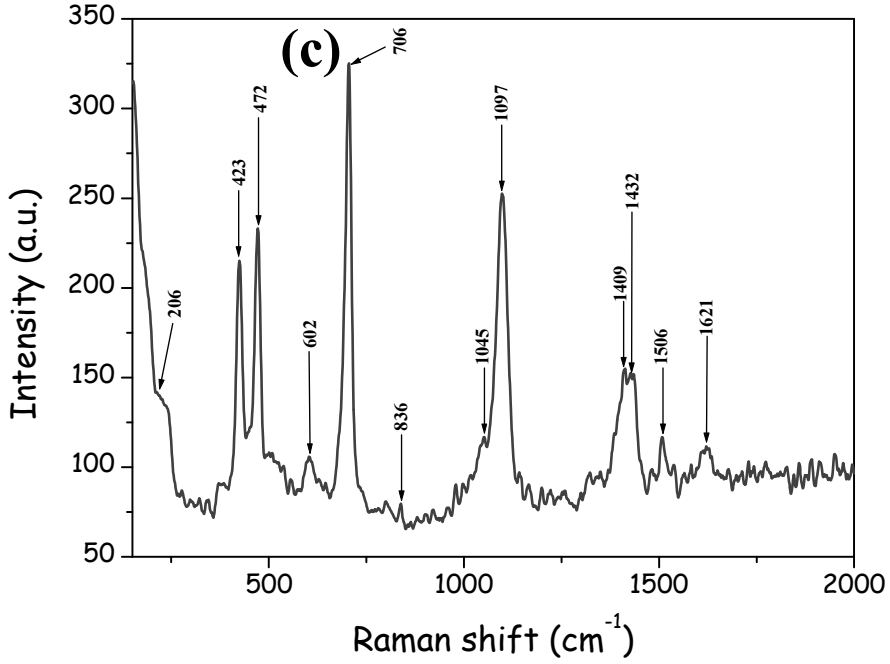

Figure S1. (c) Raman spectrum of metallogel (set I).

Discussion

Figure S1a shows the FTIR spectrum of thiourea molecule and the xerogels (resulted from the drying of the as synthesized gel) in single window. The N−H stretching mode of the parent thiourea molecule arises as strong and broad signals in the 3000-3500 cm^{-1}. Similar band positions for the xerogel indicates that metal ion coordination have an insignificant effect on the above stretching mode. However its corresponding bending vibration in the xerogel occurs at ~1626 cm^{-1} w.r.t ~1618 cm^{-1} in pure thiourea. Thus an 8 cm^{-1} shift is noticed indicating the hydrogen bonded nature of the −NH protons in the gel matrix. Clear alterations in spectral profiles are noticed for the 'C−N' and 'C=S' vibrational modes in relation to their positions and relative intensities. The first mode, appearing at ~1474 and ~1085 cm^{-1}, is relatively blue shifted (to ~1510 and ~1106 cm^{-1}) but with a significant lowering in intensities. Most interestingly, the narrow and sharp band at ~730 cm^{-1} (assigned to the C=S stretching vibration) experiences a considerable shift to lower wavenumber (~696 cm^{-1}) and thus gives a foolproof evidence of its reduced double bond character resulting from the ligand coordination through its sulfur atom. The above FTIR features seemingly replicate the vibrational characteristics of (1:1) 'Cu/TU' complex as repoted by Bombicz et al.[1a] Figure S1a also suggests the similar vibrational behaviour of the xerogels having different compositional ratio. Additionally, the IR spectra of both the xerogels of the chloride and bromide analogues (Figure S1b) having same stoichiometry are markedly comparable suggesting their isostucturality. Figure S1c is the Raman spectrum of

the xerogel. The characteristic $\nu_{(C=S)}$ band appearing at ~706 cm^{-1} (which appear at ~732 cm^{-1} for free thiourea molecule) again authenticates the reduced double bond nature of the thione moiety owing to its Cu(II) coordination through the sulfur atom. No splitting was observed for this intense signal indicating only the bridging mode of coordination of thiourea throughout the structural unit.[1b,c] Finally the presence of a weak signal at ~206 cm^{-1} is the birthmark of $\nu_{(Cu-S)}$ mode and in fact, is the evidence of tetra-coordinated metal centres (as for tri-coordination the signal appears at higher wavenumber).

References:

1. (a) Bombicz, P.; Mutikainen, I.; Krunks, M.; Leskelä, T.; Madarász, J.; Niinistö, L. Synthesis, Vibrational Spectra and X-ray Structures of Copper(I) Thiourea Complexes. *Inorg. Chim. Acta* **2004**, *357*, 513-525. (b) Bowmaker, G. A.; Hanna, J. V.; Pakawatchai, C.; Skelton, B. W.; Thanyasirikul, Y.; White, A. H. Crystal Structures and Vibrational Spectroscopy of Copper(I) Thiourea Complexes. *Inorg. Chem.* **2009**, *48*, 350-368. (c) Bott, R. C.; Bowmaker, G. A.; davis, C. A.; Hope, G. A.; Jones, B. E. Crystal Structure of $[Cu_4(tu)_7](SO_4)_2]\cdot H_2O$ and Vibrational Spectroscopic Studies of Some Copper(I) Thiourea Complexes. *Inorg. Chem.* **1998**, *37*, 651-657.

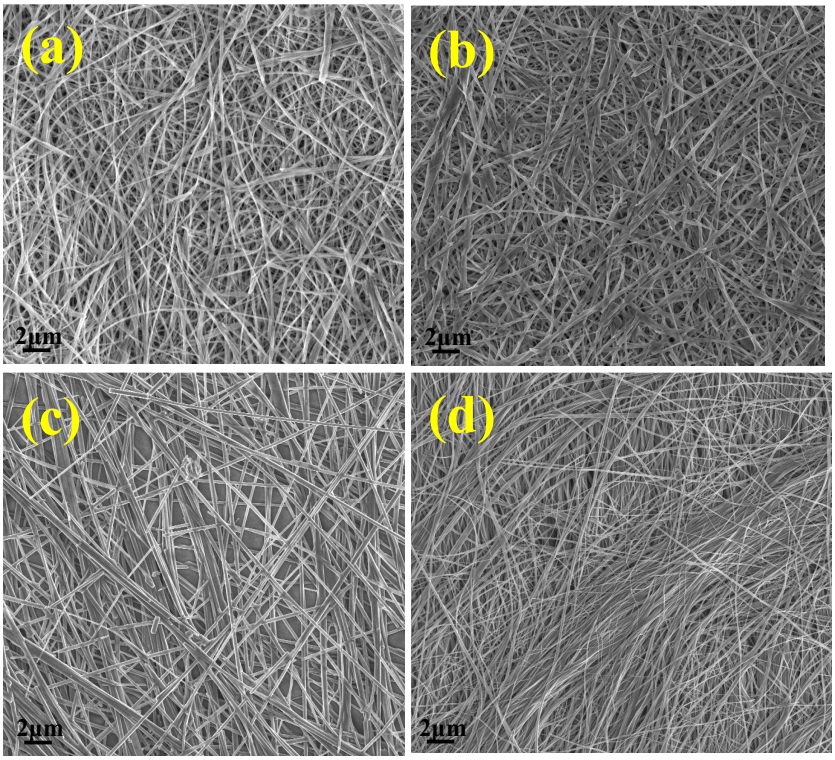

Figure S2. FESEM images of metallogel of (a) set III (b) set V (c) set VII and (d) set IX.

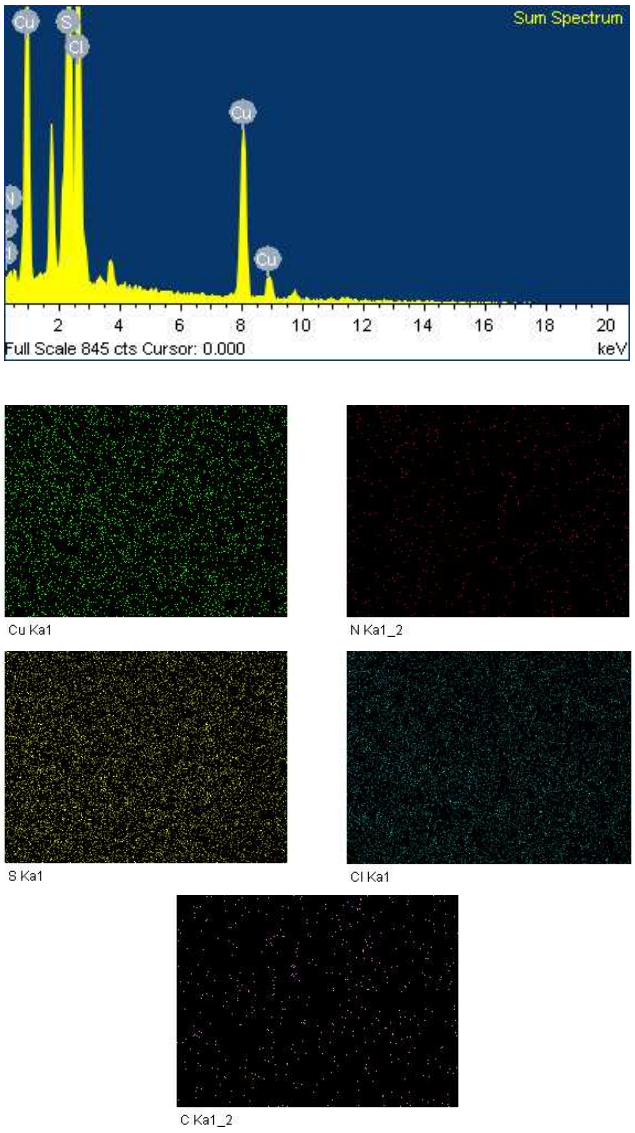

Figure S3. EDX pattern and elemental mapping analysis of metallogel showing the presence of Cu, S, N, Cl and C as the constitutional elements (set I; chloride analogue).

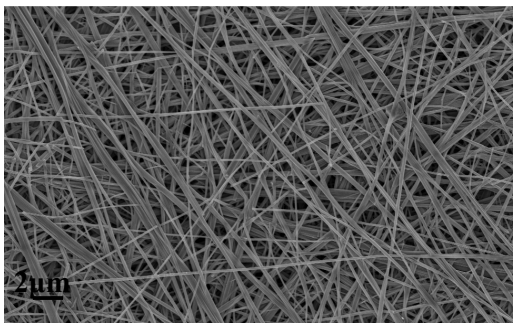

Figure S4. FESEM image of xerogel (set I; chloride analogue).

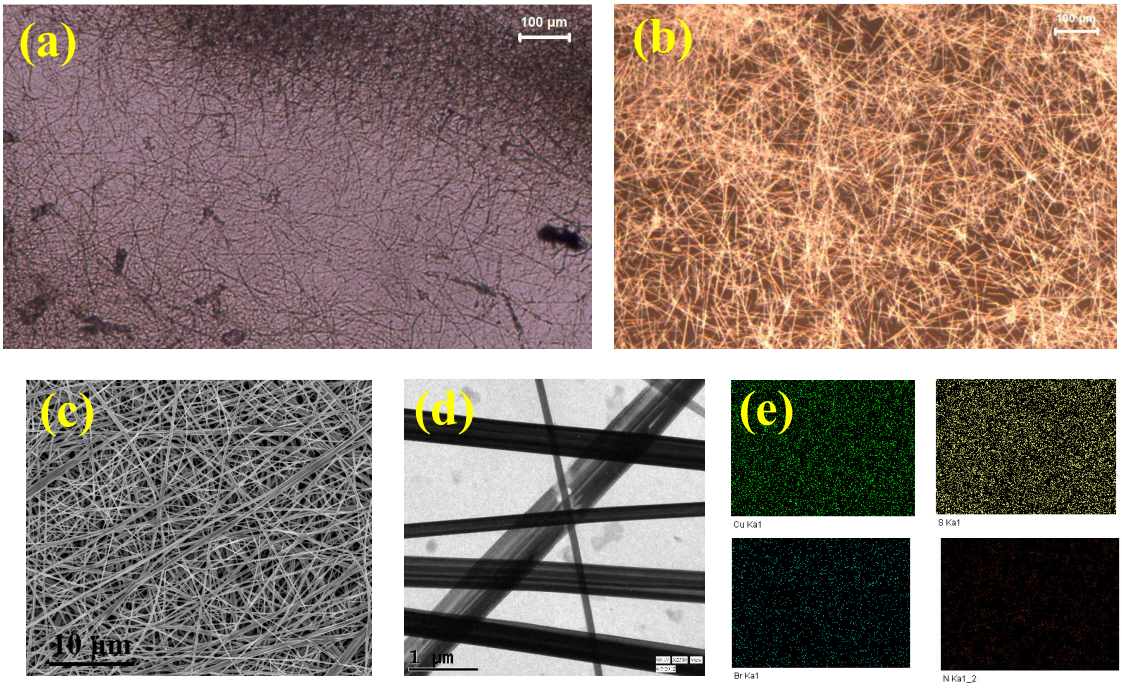

Figure S5. POM images of xerogel (set I) (a) chloride analogue (b) bromide analogue. (c) FESEM image (d) TEM image and (e) elemental mapping analysis of xerogel (set I; bromide analogue).

Effect of Interfering ions

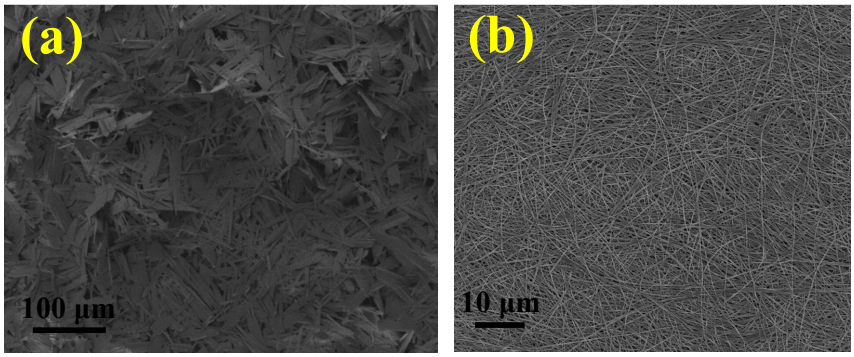

Figure S6. FESEM image of the metallogel after (a) $HgCl_2$ and (b) $CdCl_2$ treatment.

Discussion

The synthesized metal-organic gel shows chemical response towards some selective metal ions and anions. For example, addition of Hg^{2+} salt (eg. $HgCl_2$, $HgBr_2$ etc.) in the preformed metallogel results in its immediate transformation to a sol with the concomitant formation of insoluble HgS. The network structure subsequently changes to

a flake like nanostructure (Figure S6a). However the other thiophilic congeners (Pb^{2+}, Zn^{2+} and Cd^{2+} salt) could not bring such physical change and hence in morphology (Figure S6b). Here it is worth mentioning that Bi^{3+} and Sb^{3+} salts were also able to disrupt the gel through more favourable formation of their insoluble sulphides (K_{sp} = $2x10^{-53}$ for HgS; $1.1x10^{-73}$ for Bi_2S_3; $1.6x10^{-93}$ for Sb_2S_3). In fact the highly negative solubility product values (K_{sp} = $2x10^{-53}$ for HgS; $1.1x10^{-73}$ for Bi_2S_3; $1.6x10^{-93}$ for Sb_2S_3) of these sulphides endorse the irreversible breaking of the metallogel. Similarly, some selective anions (CN^-, I^-, S^{2-}, SCN^-) when added as their sodium/potassium salt also caused the irreversible gel-sol transformation either through complexation (with CN^-, forming stable teracyanocuprate ion) or through formation of insoluble complex (with I^-, S^{2-} and SCN^- forming CuI, Cu_xS_y and CuSCN respectively). In literature there are few reports on ion-triggered depolymerisation of gel frameworks. For instances, fluoride ion induced gel-sol transition has been recently reported by different research groups for a variety of amide functionalized organogel systems where the fluoride ion assisted deprotonation of the 'amide-proton' has been shown responsible for the phase transition. Similar ion-responsive behaviour has also been observed for few metallogel systems.[2]

References:

2. (a) Liu, J. –W.; Yang, Y.; Chen, C. –F.; Ma, J. –T. Novel Anion-Tuning Supramolecular Gels with Dual-Channel Response: Reversible Sol−Gel Transition and Color Changes. *Langmuir* **2010**, *26*, 9040-9044. (b) Zhang, Y. –M.; Lin, Q.; Wei, T. –B.; Qin, X. –P.; Li, Y. A novel smart organogel which could allow a two channel anion response by proton controlled reversible sol–gel transition and color changes. *Chem. Commun.* **2009**, *45*, 6074-6076. (c) Džolić, Z.; Cametti, M.; Cort, A. D.; Mandolini, L.; Žinić, M. Fluoride-responsive organogelator based on oxalamide-derived anthraquinone. *Chem. Commun.* **2007**, *43*, 3535-3537. (d) Wang, C.; Zhang, D.; Zhu, D. A Chiral Low-Molecular-Weight Gelator Based on Binaphthalene with Two Urea Moieties: Modulation of the CD Spectrum after Gel Formation. *Langmuir* **2007**, *23*, 1478-1482. (e) Rajamalli, P.; Prasad, E. Low Molecular Weight Fluorescent Organogel for Fluoride Ion Detection. *Org. Lett.* **2011**, *13*, 3714-3717. (f) Xing, L. –B.; Yang, B.; Wang, X. –J.; Wang, J. –J.; Chen, B.; Wu, Q.; Peng, H. –X.; Zhang, L. –P.; Tung, C. –H.; Wu, L. –Z. Spontaneous Fiber Formation and Hydrogelation of Nucleotide Bolaamphiphiles. *Langmuir* **2013**, *29*, 2843-2848. (g) Kim, H. –J.; Lee, J. –H.; Lee, M. Stimuli-Responsive Gels from Reversible Coordination Polymers. *Angew. Chem. Int. Ed.* **2005**, *44*, 5810-5814. (h) Xing, B.; Choi, M. –F.; Zhou, Z.; Xu, B. Spontaneous Enrichment of Organic Molecules from Aqueous and Gas Phases into a Stable Metallogel. *Langmuir* **2002**, *18*, 9654-9658.

Stimuli responsive behaviour

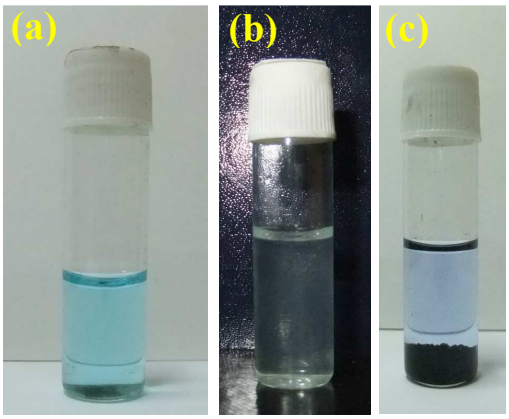

Figure S7. Digital image showing the responsive behaviour of the metallogel with external stimuli: (a) Disodium salt of ethylenediaminetetracetic acid (b) hydrogen peroxide and (c) ammonia.

Discussion

Some selected external stimuli can affect the molecular gelation when the gel is exposed to the chemical agents. These include H_2O_2, NH_3 and disodium salt of ethylenediaminetetracetic acid (Na_2EDTA). An irreversible transformation from gel to sol phase was observed in all these cases (Figure S7). This chemical response resulted either due to the favoured metal-chelation (for Na_2EDTA) or owing to the oxidation of the sulfur containing ligand system (for H_2O_2). And for NH_3, it raises the pH of the medium, resulting in an immediate formation of a black precipitate (of Cu_2S). Other amine ligands (eg. Et_3N, $NH_2CH_2CH_2NH_2$, $OHCH_2CH_2NH_2$ etc.) could similarly replicate the above result. Such stimuli controlled gel-sol transformation has been recently reported for few other Cu(II) metallogel systems.[3]

References:

3. (a) Samai, S.; Biradha, K. Chemical and Mechano Responsive Metal-Organic Gels of Bis(benzimidazole) based Ligands with Cd(II) and Cu(II) Halide Salts: Self Sustainability and Gas and Dye Sorptions. *Chem. Mater.* **2012**, *24*, 1165-1173. (b) Džolić, Z.; Cametti, M.; Milić, D.; Žinić, M. The Formation of $CuCl_2$-Specific Metallogels of Pyridyloxalamide Derivatives in Alcohols. *Chem. Eur. J.* **2013**, *19*, 5411-5416.

pH effect

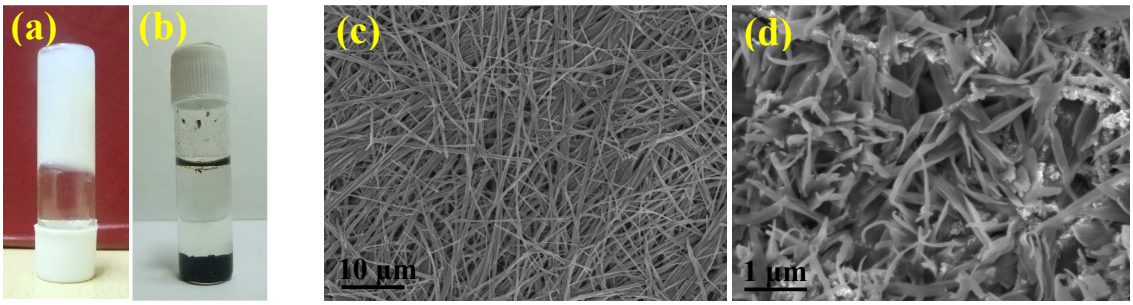

Figure S8. Digital images showing the response of the metallogel when treated with (a) 0.1 M HCl and (b) 0.1 M NaOH. FESEM images of the (c) acid treated and (d) alkali treated metallogel. These results clearly suggest the sustainability of the gel frameworks in acidic pH but rupture of the fibrous structure in an alkaline pH.

Discussion

The gel material was found to retain its stability only in acidic and neutral pH condition (as confirmed by the 'vial-inversion' practice) owing to the higher degree of protonation of the amine functionality of the thiourea/disulfide ligands which in turn promotes an extensive cross-linking through hydrogen bonding to stabilize the supramolecular assembly. However in alkaline pH, the successive deprotonation cause the breaking of the assembly to result in an immediate and irreversible transformation of the gel to a sol phase (Figure S8a and b). Again, this higher pH of the medium also favours the precipitation of black copper sulphide. Such pH regulated assembly-disassembly has been illustrated for the metallo-hydrogel systems of melamine/glutathione/N-acetyl-L-cysteine and few other gelators.[4]

References

4. (a) Casuso, P.; Carrasco, P.; Loinaz, I.; Cabañero, G.; Grande, H. J.; Odriozola, I. Argentophilic hydrogels: elucidating the structure of neutral *versus* acidic systems. *Soft Matter* **2011**, *7*, 3627-3633. (b) Bairi, P.; Roy, B.; Nandi, A. K. pH and anion sensitive silver(I) coordinated melamine hydrogel with dye absorbing properties: metastability at low melamine concentration. *J. Mater. Chem.* **2011**, *21*, 11747-11749.

X-ray diffraction

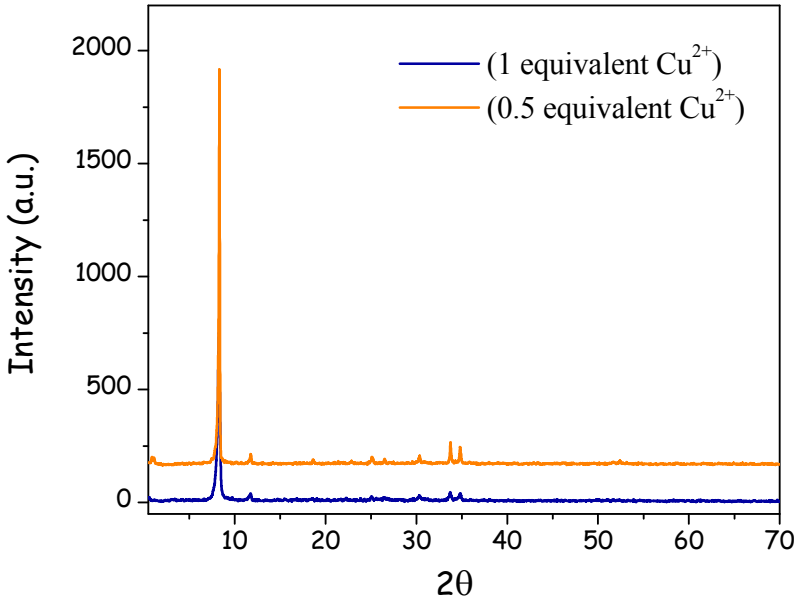

Figure S9. XRD patterns of the dried metallogels
(of set I and set VI respectively; chloride analogue).

Discussion

The well crystalline nature of the dried xerogel was assured from its XRD pattern. The small angle X-ray diffraction (SAXD) pattern showing high-intense diffraction peak at 2θ = 8.2˚ represents its polymeric nature (Figure S9). The patterns of the chloride and bromide analogues having same stoichiometry differ from each other indicating a difference in their crystal habits.

Absorption-emission behaviour

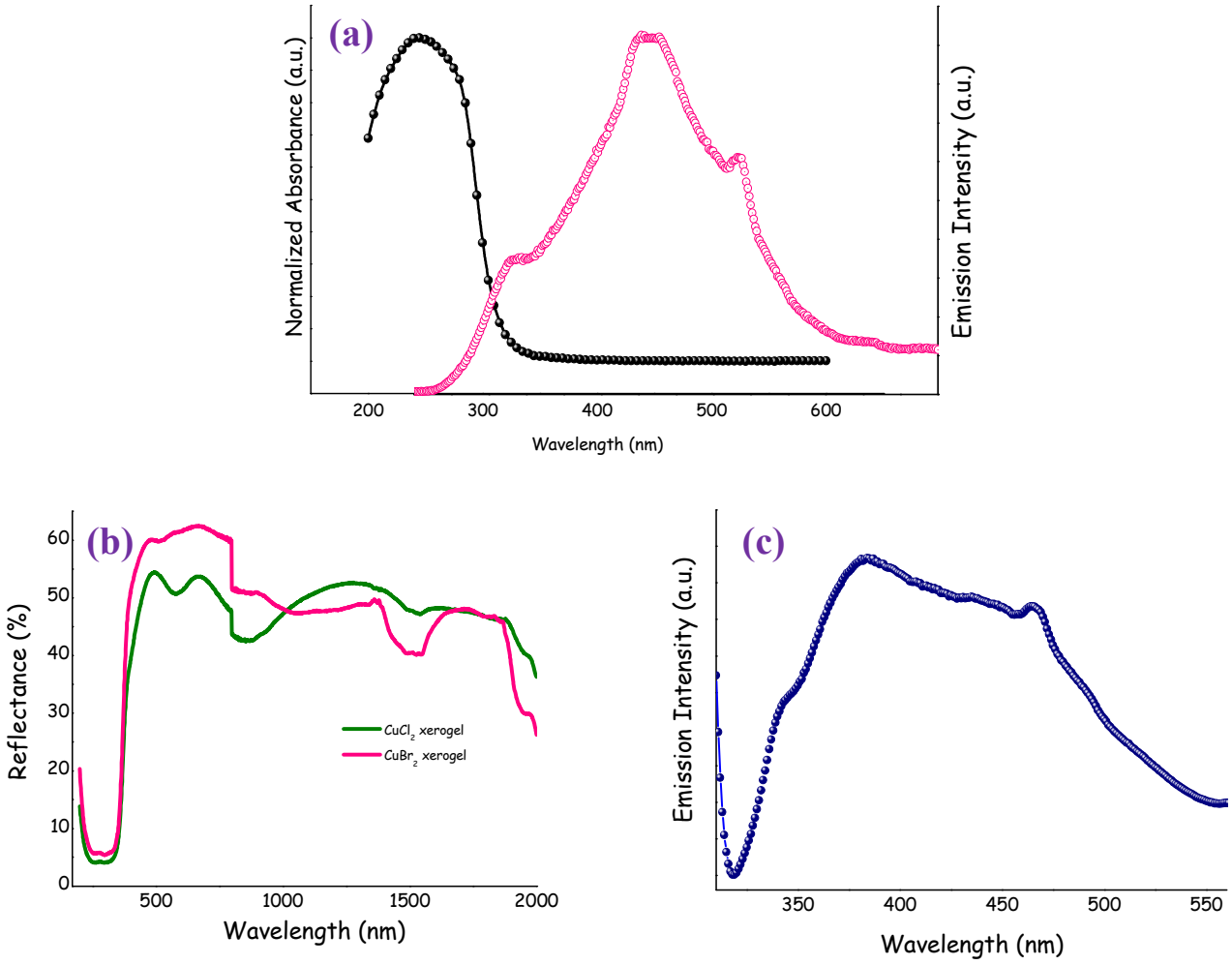

Figure S10. (a) Absorption-emission profile of the metallogel in its well dispersed condition in aqueous medium. (b) DRS spectra of the chloride and bromide xerogels. (c) Solid state emission spectrum of the xerogel (set I; chloride analogue; λ_{ex} = 290 nm).

Discussion

Figure S10a presents the absorption-emission profile of the metallogel in its well dispersed condition in aqueous medium. We observed a strong emission from the material at ~410 nm (λ_{ex} = 245 nm) which could be a consequence of MLCT $d^{10} \rightarrow d^{9}\pi^{*}$ transitions.[5] And the enhanced fluorescence in the matrix can be rationalized in view of the gel-phase confinement of the fluorescent structural units.[5] The solid state reflectance spectra of the chloride and bromide xerogels are shown in Figure S10b (λ_{max} = 290 nm). Therefore ~45 nm blue-shift was observed

for the gel in its aqueous dispersion. Strong emission was also observed in the xerogel phase (Figure S10c). A recent study by Chattopadhyay et al. has reported a similar photoluminescence response from a Cu(I) coordination polymer bearing a 'Cu_2S_2' core.[5e]

References:

5. (a) Rath, N. P.; Holt, E. M. Tanimura, K. Fluorescent Copper(I) Complexes: Structural and Spectroscopic Characterization of bis(p-toluidine)bis(acetonitrile)tetraiodotetracopper and bis[(p-chloroaniline)(acetonitrile)diiododicopper] tetrameric complexes of mixed-ligand character. *Inorg. Chem.* **1985**, *24*, 3934-3938. (b) Hao, L.; Mansour, M. A.; Lachicotte, R. J.; Gysling, H. J.; Eisenberg, R. Oxidative additions and luminescence involving iridium-gold-iridium chains formed by binding of gold(I) to the metallamacrocycle $Ir_2Cl_2(CO)_2$[.mu.-$Ph_2PCH_2As(Ph)CH_2PPh_2]_2$. *Inorg. Chem.* **2000**, *39*, 5520-5529. (c) Rajamalli, P.; Prasad, E. *Langmuir* **2013**, *29*, 1609-1617. (d) Leong, W. L.; Batabyal, S. K.; Kasapis, S.; Vittal, J. J. Tunable Morphology and Mesophase Formation by Naphthalene-Containing Poly(aryl ether) Dendron-Based Low-Molecular-Weight Fluorescent Gels. *Chem. Eur. J.* **2008**, *14*, 8822-8829. (e) Jana, S.; Bhowmik, P.; Chattopadhyay, S. Unique *in situ* reduction of copper(II) forming an interesting photoluminescent stair-polymer of copper(I) with a Cu_2S_2 core. *Dalton Trans.* **2012**, *41*, 10145-10149.

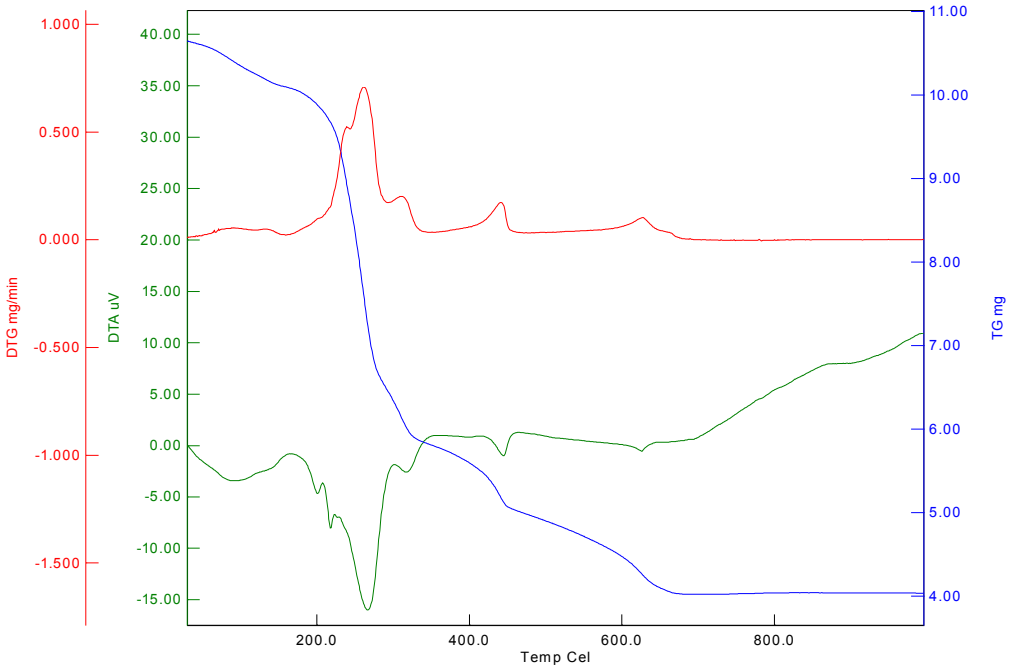

Figure S11. Thermogram of the gel.

Redox-switchability

Figure S12. $K_2Cr_2O_7$ mediated oxidative dissolution (performed in slight HCl medium) of the metallogel as shown in stepwise manner [(i)-(vi)] and gradual regeneration of the gel material from the oxidized sol phase upon addition of ascorbic acid [(vii)-(xiii)].

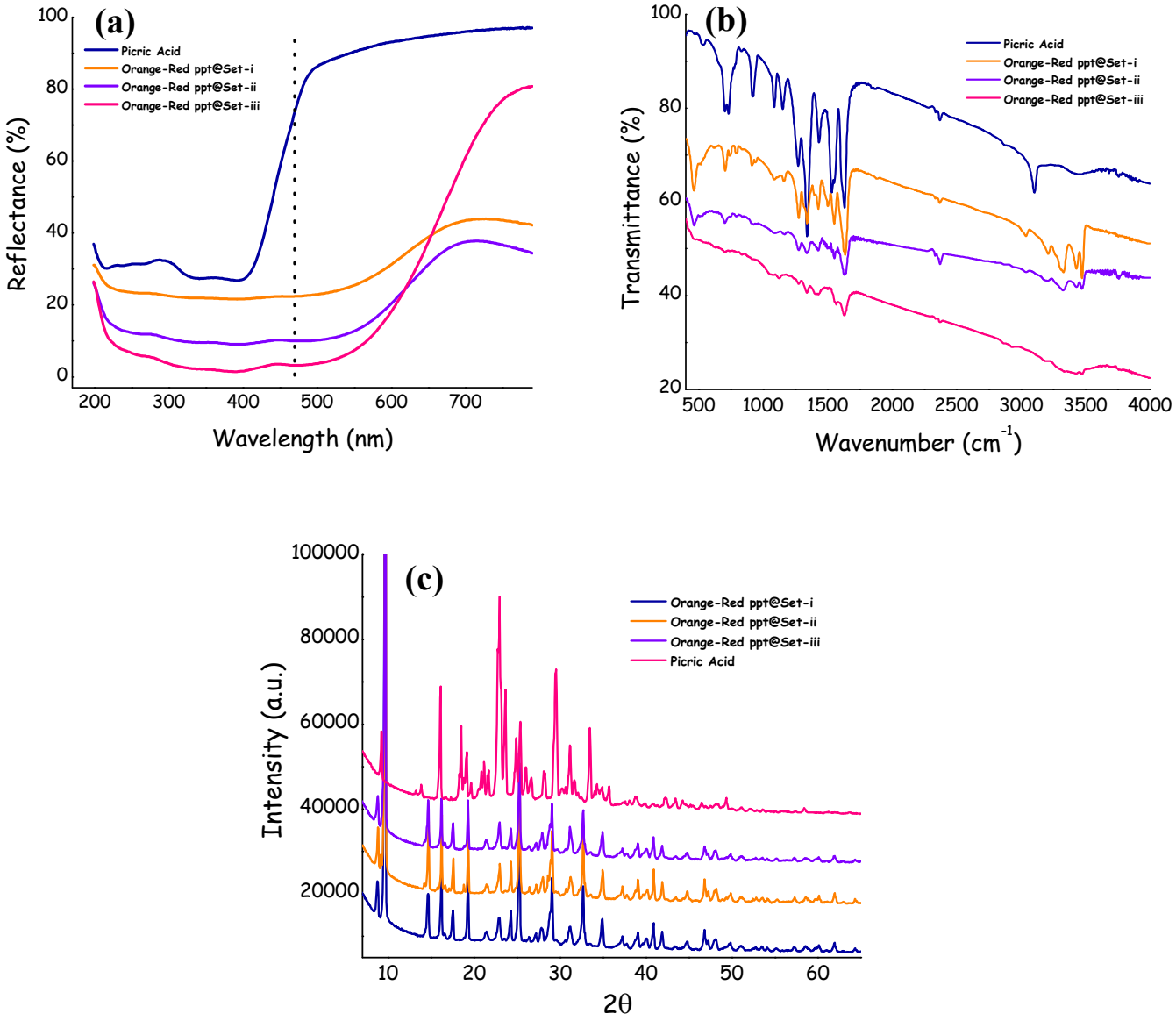

Figure S13. (a) DRS spectra (b) FTIR spectra and (c) XRD patterns of picric acid and the orange-red precipitates (collected from set i, ii and iii).

Rheology

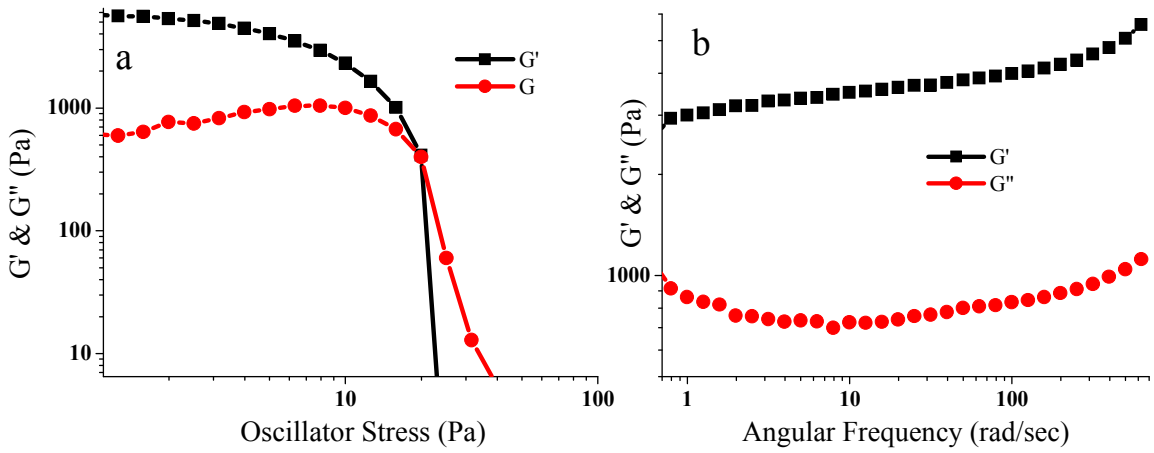

Figure S14. (a) Storage (G′) and Loss (G″) modulus vs. oscillator stress at constant frequency 1 Hz (b) Storage (G′) and Loss (G″) modulus vs. angular frequency

Discussion

The mechanical strength of the as synthesized gel (chloride analogue; set I) has been performed using rheological experiments. On the application of stress to the gel under the metal geometry, the gel breaks down at oscillator stress. The critical stress value (yield stress) was observed to be 19.9 Pa (Figure S14a). In the gel state $G'(\omega) > G''(\omega)$ and $G'(\omega) \sim \omega^0$, where ω is the angular frequency. The dynamic frequency sweep experiments results is shown in Figure S14b. We observed that at linear viscoelastic region (LVR) both G' and G'' are almost independent of frequency changes and G' has significantly higher values than G''. This result also clearly supports the gel nature of the material though the slight and gradual increase with frequency suggests that probably solvent loss is taking place during measurement.